The Influence of Diamond Nanoparticles on Fibroblast Cell Line L929, Cytotoxicity and Bacteriostaticity of Selected Pathogens

Katarzyna Mitura [1,2,*], Joanna Kornacka [1], Aleksandra Niemiec-Cyganek [3], Lucyna Pawlus-Łachecka [3,4], Katarzyna Mydłowska [1], Anna Sobczyk-Guzenda [5], Witold Kaczorowski [5], Paulina Ossowska [1], Błażej Bałasz [1] and Piotr Wilczek [3,4]

[1] Faculty of Mechanical Engineering, Technical University of Koszalin, Racławicka 15-17, 75-620 Koszalin, Poland; joanna.kornacka@s.tu.koszalin.pl (J.K.); katarzyna.mydlowska@tu.koszalin.pl (K.M.); paulina.ossowska97@gmail.com (P.O.); blazej.balasz@tu.koszalin.pl (B.B.)

[2] Faculty of Mechanical Engineering, Faculty of Materials Science, Technical University of Liberec, 461-17 Liberec, Czech Republic

[3] Prof. Zbigniew Religa Foundation for Cardiac Surgery Development, Wolności 345a, 41-800 Zabrze, Poland; ancyganek@gmail.com (A.N.-C.); mikrob@frk.pl (L.P.-Ł.); mildes@post.pl (P.W.)

[4] Faculty of Health Sciences, Calisia University, Nowy Świat 4, 62-800 Kalisz, Poland

[5] Faculty of Mechanical Engineering, Institute of Material Sciences and Engineering, Lodz University of Technology, Stefanowskiego 1/15, 94-924 Lodz, Poland; anna.sobczyk-guzenda@p.lodz.pl (A.S.-G.); witold.kaczorowski@p.lodz.pl (W.K.)

* Correspondence: katarzyna.mitura@tu.koszalin.pl

Abstract: The main problem with using modified allotrophic forms of carbon with nanodiamond particles in the production of food packaging is establishing the boundary between safety, as it affects the human body, and the adequate and effective action of the substances. One vital area of concern is the transmission of pathogens in food into the body. The aim of this study was to evaluate the cytotoxicity and bacteriostatic biological activity of two different modifications of diamond nanoparticles: pure detonation nanodiamond particles (DND) obtained by Danienko and plasma-chemically modified detonation nanodiamond particles obtained by the microwave plasma activated chemical vapor deposition method in a rotary chamber (MDP1) An indirect method was used to evaluate the cytotoxicity effect in accordance with ISO 10993–5. The viability of the L929 fibroblast cell line used as a control was 98.5%, for DND 95.14%, and the lowest level of viability for MDP1 was 88.63%. *Escherichia coli* and *Staphylococcus aureus* bacteria were used in bacteriostatic tests and the degree of cytotoxicity of the tested materials was classified as low. The in vitro cytotoxicity results indicate no toxic effect on L929 cells nor any effect on any of the samples tested against the bacterial strains us

Keywords: diamond nanoparticles; cytotoxicity; bactericidal properties; scanning electron microscope (SEM); X-ray diffraction (XRD); Raman spectroscopy; FT–IR spectroscopy

1. Introduction

Detonation nanodiamonds (DND), or alternatively UDD (Ultradispersed Diamond,) are diamond products obtained in the process of carbon detonation during the explosion of the TNT/RDX explosive mixture (TNT/hexogen–1,3,5–Trinitroperhydro–1,3,5–triazine). Detonation nanodiamond particles with a diameter of several nanometers, are formed as a result of detonative synthesis [1–3].

The single grain size specification of the individual particles provided by the Adamas Nanotechnologies Company range from 2 to 4 nm. Nanodiamonds not only have all the features of a diamond, but have all the characteristics of powders, such as high entropy

and good chemical and biological activity Detonation nanodiamonds have a very highly developed surface, which results from their very small grain size, hybridization of δ sp³ of carbon atoms and the contents of diamond phase over graphite phase. Due to the presence of free bonds on the surface of detonation nanodiamonds, they form agglomerates. which can reach micrometric sizes, but still have a very high surface activity. For this reason, it is very interesting to modify the surface of nanodiamonds, e.g., with plasma-chemical methods; these modifications affect the size of the agglomerates, the content of the diamond phase, and the type of functional groups on the surface of nanodiamonds. There are known solutions created using a static plasma chemical reactor chamber which are widely used in the surface modification of materials with plasma activated chemical vapor deposition (MW PACVD) [2–5].

The nanodiamonds produced have a lot of interesting advantages, for example, high stability in corrosive media, being chemically inert, optically transparent, and also biocompatible. Several publications have proved that the nanodiamonds do not induce significant cytotoxicity in a variety of animal/human cell types [4,5].

Diamond nanoparticles that do not show cytotoxicity can be used in regenerative medicine and tissue engineering as nano-scaffolds. Most often it is utilized as multifunctional bone nano-scaffolds consisting of biopolymers modified with diamond nanoparticles which have no cytotoxic effect on osteoblasts and do not disturb the proliferation of these cells [5–8]. Diamond nanoparticles are practically nontoxic. Carbon nanoparticles have been identified as stable, fluorescently labeled tumor cell lines and it has been concluded that the labeled cells are suitable for drug cytotoxicity tests. [9].

The cytotoxicity of detonation nanodiamond particles for urothelial cells and the routes of their internalization remains an open question in the aspect of nanodiamond usage. Detonation nanodiamonds entered the urothelial cells, but did not induce any significant cytotoxic effects on either normal or cancer urothelial cells in vitro. These results support the potential of DNDs to be researched as a nontoxic delivery system for urological applications [10].

The antibacterial properties of nanodiamond materials have also been examined. Antibacterial activity would increase the attractiveness of nanodiamonds as a platform for developing biomaterials. Many publications have described an antibacterial effect of some (nano)diamonds Their interaction with bacteria has been linked to chemical surface groups on the diamond [11–14].

Surface functionalization of nanodiamonds allows the possibility of producing an active biological and chemical surface. The presence of functional groups on the nanodiamond surface determine its antibacterial properties and non-cytotoxic effects. Detonation nanodiamonds can be modified to broaden the array of their therapeutic applications. The functionalization of nanodiamond particles could be affected in two ways, i.e., doping and surface functionalization. [15–17].

One of the dangers for humans is the transmission of pathogens, which can enter the body through food, causing disease. Therefore, it is important to study diamond nanoparticles and other carbon allotropes in terms of their antimicrobial properties which do not produce a toxic effect on cellular lines and tissue structures [4,18–24].

2. Materials and Methods

2.1. Cytotoxicity

Pure detonation nanodiamond particles (DND) were manufactured by the Danilenko method and a single grain size was estimated at about 2–4 nm [1]. The single grain size specification of the individual particles provided by the Adamas Nanotechnologies Company range from 2 to 4 nm. Plasma-chemically modified detonated nanodiamond (MDP1) was manufactured in the Koszalin University of Technology using the MW/RF PACVD method in a rotary chamber [2].

The cytotoxicity of the samples was evaluated by indirect contact assays. The first step in sample preparation was their sterilization in an antibiotic bath for 24 h at 4–8 °C.

The samples for the study were placed in a 0.1 g/mL extraction medium. Extraction was carried out at 37 °C for 24 h under constant agitation.

Evaluation of the cytotoxicity effects was performed by an indirect method in accordance with ISO 10993–5. The fibroblast line, clone L929–American Type Culture Collection (ATCC), was used for this study. Cells were cultured under standard conditions in Medium 199 supplemented with 10% FCS. It was essential for the assay that the cells reached 70%–80% confluence. Once adequate confluence was achieved, fresh medium was added to the culture and supplemented with an extraction medium at a ratio of 9:1. Cells were incubated under these conditions for 24 h and then stained with the vital dyes, fluorescein diacetate (FDA), and propidium iodide (PI). FDA has the ability to penetrate into cells through an intact cell membrane; once it has entered the cell it degrades to a monomer that exhibits both polar and fluorescent properties. FDA positive cells exhibit green fluorescence and are classified as viable. In contrast to FDA, PI, which exhibits red fluorescence, penetrates into cells in which the integrity of the cell membrane has been compromised. PI positive cells were classified as necrotic. Viability assessment was performed with a fluorescence microscopy technique using an inverted research microscope, AxioObserver, while AxioVision 4.8 software (Carl Zeiss) was used for image acquisition and analysis. For each repetition, the numbers of live and necrotic cells in the field of view, a rectangle with sides of 340 μm × 255 μm, were counted. In addition to counting the number of necrotic cells, the morphology of viable, adherent cells and any differences in cell density were observed. According to this data, a classification of the cytotoxicity of tested samples was performed (Table 1)

Table 1. Qualitative morphological classification of cellular cytotoxicity according to ISO 10993–5 standards.

Degree of Cytotoxicity	Reactivity	Cell Condition
0	not available	Discrete intra-plasmatic granules, no lysis, no reduction in cell growth.
1	slight	No more than 20% round cells, loosely suffused without intracytoplasmic granules, showing morphological changes, few cell lysis, little inhibition of cell growth.
2	mild	Not more than 50% round, devoid of intra-plasmacytic granules, strong cell lysis, not more than 50% inhibition of cell growth.
3	moderate	Not more than 70% of surface containing round cells and lysed, not completely damaged, cell growth inhibition greater than 50%.
4	strong	Almost complete and total cell destruction

According to the guidelines, the following classification of materials is adopted:

For each microscopic image, the number of live and dead cells were counted using ImageJ software. Statistical analysis of the results obtained was performed using the Jamovi program. The normality of the distribution was verified using the Shapiro–Wilk test, whereas homogeneity of variance was verified using Levene's test. In the case of samples which did not meet the assumption of normality of distribution, the Box–Cox transformation was applied. Samples fulfilling assumptions of normality of distribution were subjected to one-way analysis of variance (ANOVA).

2.2. Bacteriostaticity

Samples were placed in sterile FALCON type tubes and 1 mL of NaCl 0.9% was added to each. Extraction was carried out in a shaker at about 150 rotation/min. Each sample, after extraction, was centrifuged and filtered using a syringe filter (CORNING Ø 0.45 μm). The resulting extract was used for bacteriostatic tests. The bacteriostatic/bactericidal effect

was evaluated using "in house" strains of *Escherichia coli* and *Staphylococcus aureus* by the disk diffusion method on Müller–Hinton Agar. A bacterial suspension with a density of 0.5 McFarland (1–2.9 × 108 cfu) was prepared according to accepted standards.

Each sample was tested in 3 replicates with each bacterial strain. Test samples were 10 and 20 µL extract soaked discs, the (−) negative control was a NaCl 0.9% soaked disc, (+) positive controls were standard antibiotic discs (gentamicin, levofloxacin). Table 2 shows the weight of carbon nanomaterials after the extraction process.

Table 2. Samples were appropriately weighed for testing.

Type of Powder	Amount of Sample Weighed
DND	0.051 g
MDP1	0.026 g

2.3. SEM

The SEM analysis enables the morphology to be estimated, i.e., fragmentation, dispersion shape, and to transfer the possibility of creating developed surfaces, showing high biological activity of nanodiamond surfaces. The samples were placed on a special tripod, thanks to which it was possible to set the proper position and angle of inclination. A very low vacuum (LV) was present in the chamber. A scanning electron microscope (SEM) JSM–5500 LV, from Jeol Ltd. (Peabody, MA, USA) was used.

2.4. XRD

An X'Pert Panalytical powder diffractometer (Malvern Panalytical, Malvern, UK) was used for the X-ray diffraction (XRD) study. The radiation source is an X-ray tube with a linear focus. The measurement was performed using a copper anode (CuKα radiation beam, λ = 1.5406 Å). The samples were scanned in Bragg–Brentano geometry using a reflected beam in the 2θ 10–100° angle range using continuous rotation of the sample with a constant period T = 8 s.

2.5. Raman Spectroscopy

Raman experiments were performed on a Renishaw instrument (Gloucestershire, UK) in a Via Raman spectrometer. The spectra were observed and analyzed in the Raman shift range from 900 to 2000 cm^{-1} at an excitation wavelength of 532 nm. Then, each spectrum was de-correlated into two peaks (D and G) using spectral analysis software (Peak Fit v4.11) to calculate the ID/IG intensity ratio.

2.6. FT–IR Spectroscopy

Chemical structure analysis was carried out with the help of a ThermoScientific Nicolet INs50 FTIR spectrometer (Waltham, MA, USA) using a Seguell DRIFT reflection/scattering attachment with the variable angle of incidence of a radiation beam. Samples of carbon powders were mixed with KBr in a 1:100 proportion and placed in a holder dedicated to the reflection attachment. Measurements were carried out in an absorbance mode within the wavenumber range of 4000 to 400 cm^{-1} with a resolution of 4 cm^{-1} at the IR beam angle of 90 deg. The number of scans was equal 128 [25–27].

3. Results

3.1. Cytotoxicity Tests

The results showing the number of both live and dead cells per 1 mm^2 and the number of live cells per 1 mm^2 (Figure 1) are plotted below. Figure 1 shows that the number of dead and living cells is comparable to the control, i.e., the number of cells in the presence of carbon nanomaterials, both pure detonation powder and modified powder, practically does not change. It can be seen that in the presence of plasma-chemically modified powder (MDP1), even an increase in the number of total cells is observed. It can, therefore, be said

that modified and unmodified detonation diamond powders do not show a cytotoxic effect in presence fibroblast line, clone L929.

Assessment of the number of cells
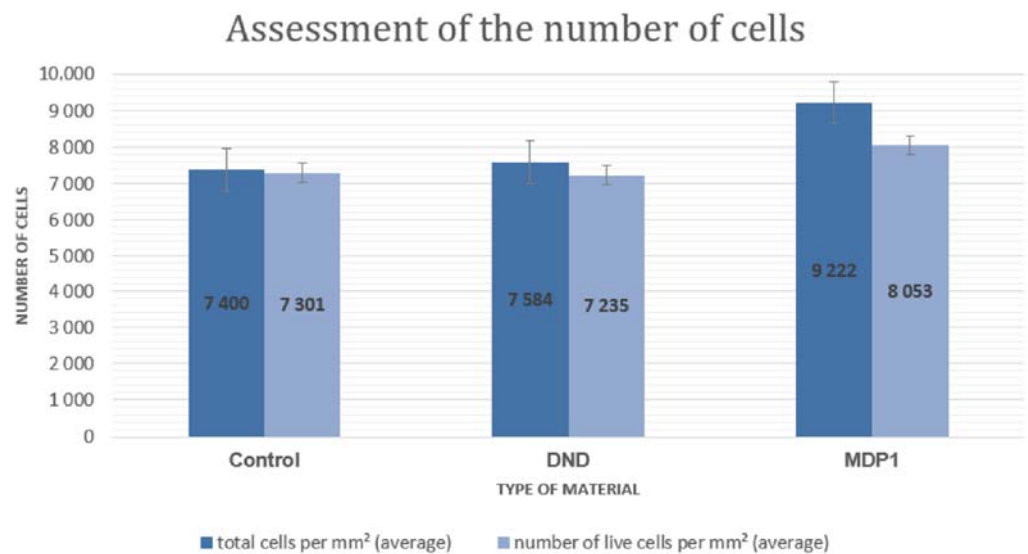
Figure 1. Assessment of the number of total cells in a given unit area and assessment of the number of live cells per unit area.

Figure 2 shows the cell viability in the presence of unmodified and plasma-chemically modified diamond nanoparticles. Cell viability was calculated from the formula:

$$viability = \frac{number\ of\ live\ cells}{number\ of\ live\ cells + number\ of\ dead\ cells} \times 100\%$$
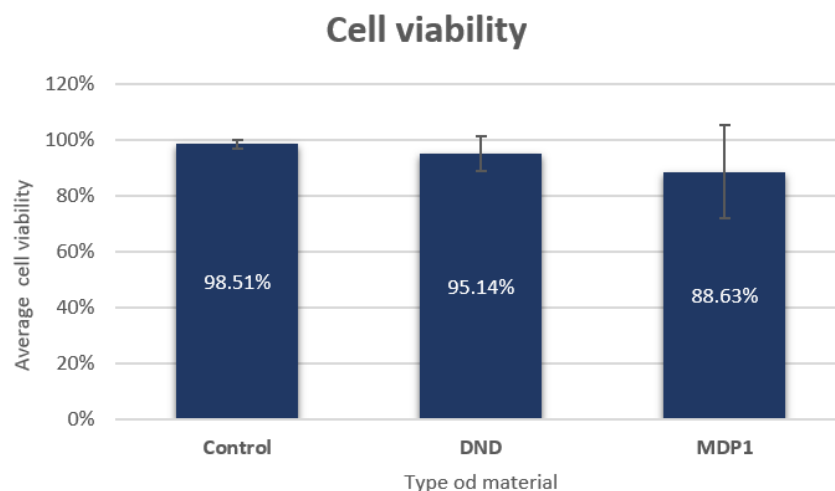
Cell viability

Figure 2. Cell viability in the presence of diamond nanoparticles.

Cell viability on the control was 98.51%, while for DND it was 95.14%, the lowest level of viable cells was achieved for MDP1 material, 88.63% (Figure 2). The degree of cytotoxicity of the tested carbon nanomaterials was classified as minor reactivity (grade 1) (Table 1). In determining the cytotoxicity of unmodified diamond nanoparticles (DND) and plasma-chemically modified diamond nanoparticles (MDP1), it was clearly observed that the degree of cytotoxicity and reactivity of the tested materials are very low. As a result of cell viability analysis, their reactivity can be determined, which in this case is low. The

nanodiamond particles tested do not cause disruption of viability and, therefore, do not have toxic effects on cells.

Figure 3 shows in all tested samples, high cell viability was observed with only single necrotic cells in the field of view. Cells showed normal morphology. There were also no significant changes in cell density.
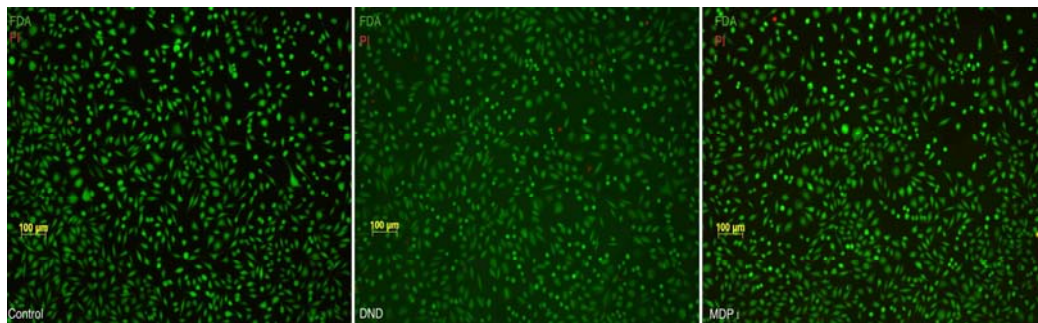
Figure 3. The pictures from the fluorescence microscope (Axio Observer [Zeiss]) show the fibroblast line, clone L929 (green fluorescense) in control without carbon nanomaterials, and in presence of DND-pure detonation nanodiamonds and plasma-chemically modified detonation nanodiamonds (MDP1).
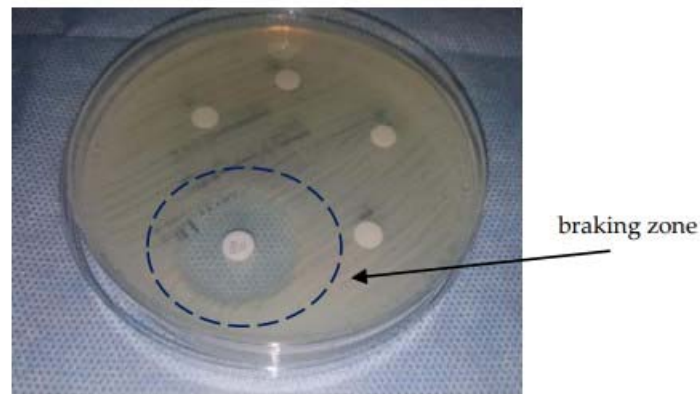
3.2. Bacteriostaticity Test

Escherichia coli and *Staphylococcus aureus* were used in bacteriostatic assays, which were performed by the disk diffusion method on Müller–Hinton Agar. Antibacterial activity was evaluated after 24 h incubation of the inoculating plates at 35 °C. Bacteriostatic effect against the bacterial strains used was observed in both samples (Figure 4a,b).

(a)　　　　　　　　　　　　　　　　　　　　　　(b)
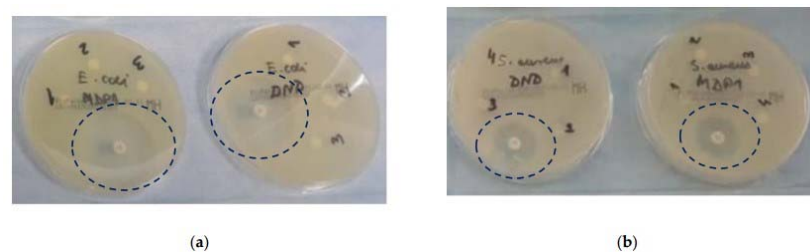
Figure 4. Bacteriostaticity assessment test of diamond nanoparticles: (**a**) MDP1 and DND test samples against *Escherichia coli* bacteria; and (**b**) MDP1 and DND test samples against *Staphylococcus aureus* bacteria.

Figure 4a,b shows no bacteriostatic effect against the bacterial strains used was observed in presence of both pathogens and carbon nanomaterials. Samples modified with pure detonation diamond nanoparticles (DND) and plasma-chemically modified diamond nanoparticles (MDP1), when tested with *Escherichia coli* (Figure 4a) and *Staphylococcus aureus* (Figure 4b), showed braking zones compared with control contains antibiotic (Figure 5). The presence of the inhibition zone in the presence of selected pathogenic strains and detonation non-modified modified diamond nanoparticles indicate small bacteriostatic nature of the carbon nanomaterials described. The visible, clear inhibition zone in the presence of the antibiotic control indicates the correctness and advisability of this test.

Figure 5. Bacteriostatic effect of a control contains antibiotic-braking zone visualized.

3.3. SEM Analysis

Figure 6a,b shows the the results of the surface morphology analysis of the carbon nanomaterials, forming agglomerates the size of micrometers, determining the sizes of the detonation plasma-chemically modified diamond powders (MDP1) and the possibility of the presence of durably bonded agglomerates (DND). A cluster of single, very small grains, forming agglomarates, can be seen, evidently the modification of the detonation diamond powder affected grain size (b). Small differences in the spherical shape of the particles can be seen, having varying sizes (91.4 nm). The study proved that the powders have a non-uniform developed surface structure. The powders presented show a well-developed specific surface area.
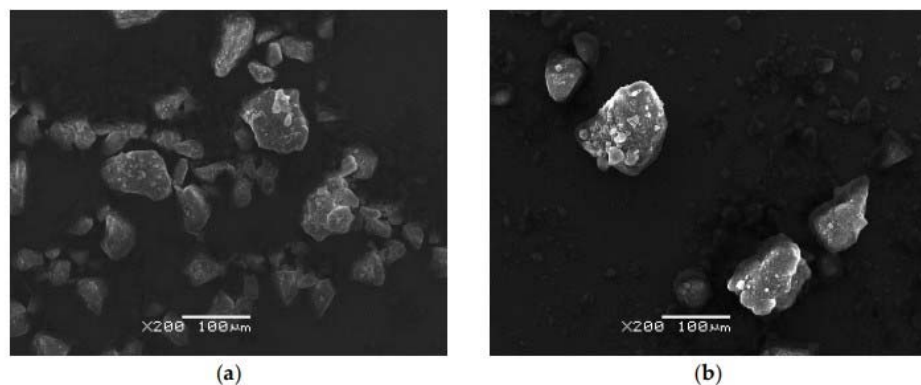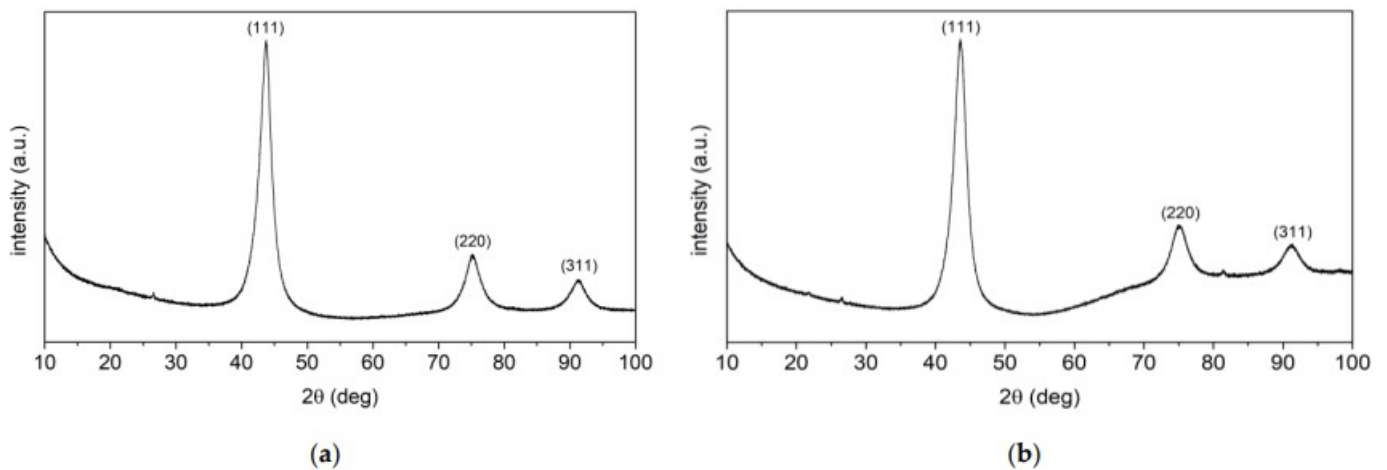

Figure 6. SEM images of diamond nanoparticles): (**a**) pure detonated nanodiamond particles (DND); and (**b**) plasma-chemically modified detonation nanodiamond particles (MDP1).

3.4. X-ray Diffraction (XRD) Analysis

XRD diffraction shows the crystallographic structure of diamond nanopowders. Analysis of the atomic structure of detonation diamond crystals proved that the nanoparticles form single crystals. Some of these monocrystals contain crystallographic defects.

The crystallographic structures of (a) unmodified detonation diamond powder and (b) plasmochemically modified diamond powder using crystal lattice parameters described in the aforementioned publications [25–28] are shown and compared in Figure 7.

In Figure 7a,b, the peaks of the diamond of each powder are shown. As a result of the modification of the nanodiamond, the crystallographic structure has not changed when compared to the unmodified nanodiamond (DND). By observing the shape of the peaks in the plasma-chemically modified nanodiamond (MDP1), amorphous carbon can be observed (b).

Figure 7. X-ray diffraction of detonation nanodiamond particles (**a**) pure detonation diamond nanoparticles DND); and (**b**) plasma-chemically modified detonation diamond powder (MDP1).

3.5. Raman Spectroscopy Analysis

In order to additionally check the content of the diamond phase in the tested diamond nanoparticles, their structure was checked by Raman spectroscopy. The greater content of the diamond phase is presented by the plasma-chemically modified detonation nanodiamond particles (MDP1) in comparison with pure detonation nanodiamond (DND) (Figure 8a,b). This is due to the plasma-chemical modification of the surface of the MDP1 powder associated with the exposure of the diamond and is expressed as a higher peak than diamond at 1319 cm^{-1}. (Figure 8b). Additionally, analysis of the nanodiamonds particles was conducted using Raman spectroscopy (Figure 8, Table 3). The ratio ID/IG = (1 + 2)/(3 + 4) was determined. MDP1 powders were determined to have higher diamond to amorphous, diamond to GLC ratio and ID/IG ratio values. Therefore, it can be concluded that in these powders, as a result of the research carried out, a certain part of DND powders underwent the graphitization process [29].
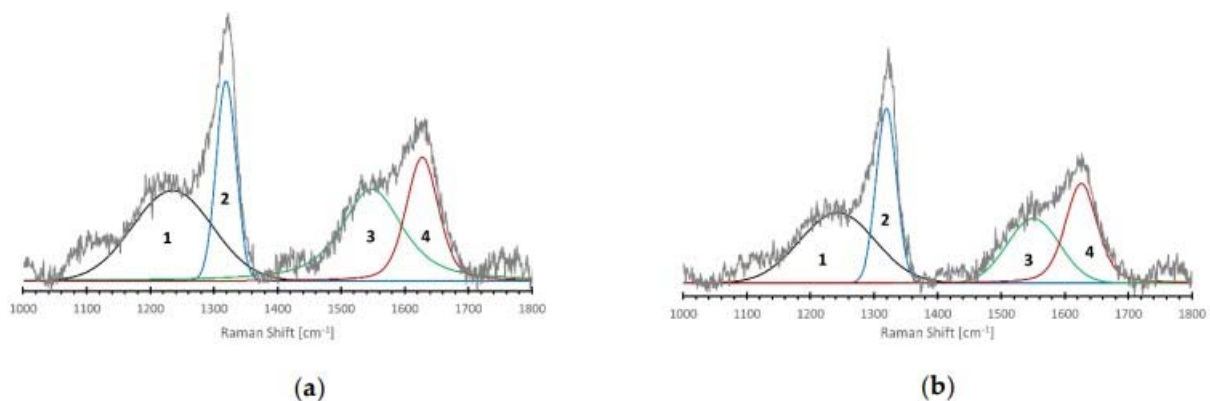
Figure 8. Raman spectroscopy images of diamond nanoparticles. (**a**) Raman spectrum of detonation nanodiamond particles manufactured by detonation method (DND)–ID/IG–0.93; and (**b**) Raman spectrum of detonation nanodiamond particles modified by the plasma-chemical method (MDP1)–ID/IG–1.24.

Table 3. Analysis of the Raman spectra.

Sample		DND	MDP1
Amorphous sp^3 peak FWHM/Position [cm^{-1}]	(1)	147/1235	139/1242
Diamond peak FWHM/Position [cm^{-1}]	(2)	37/1319	37/1319
GLS peaks FWHM/Position [cm^{-1}]	(3)	112/1548	97/1550
	(4)	59/1627	59/1625
Diamond to amorphous ratio		0.55	0.67
Diamond to GLC ratio		0.33	0.49
ID/IG		0.93	1.24

3.6. FT–IR Spectroscopy Analysis

Figure 9 shows the course of the IR spectra for tested diamond nanoparticles in the range of 4000 to 400 cm^{-1}. Additionally, Table 4 lists the locations of the most distinctly identified bands occurring in this area and the presented spectra, mainly vibrations belonging to the following bonds O–H, C–H, C=O, C–O, and C–O–C, were distinguished. Plasma-chemically modified diamond nanoparticles synthesized by the detonation method (MDP1) are characterized by the highest content of hydroxyl groups (–OH groups). The presence of carbonyl groups (C=O) is revealed in the band at 1724 cm^{-1}, and the wide peak at 3448 cm^{-1} is attributed to the O–H stretching vibrations of the C–OH groups and may also be related to the presence of water in this material. The intense peak belonging to the C=O groups is in the spectrum of pure detonation nanodiamond (DND). Additionally, for both detonation nanodiamonds, intense peaks originating from the C–O groups were observed [30–32].
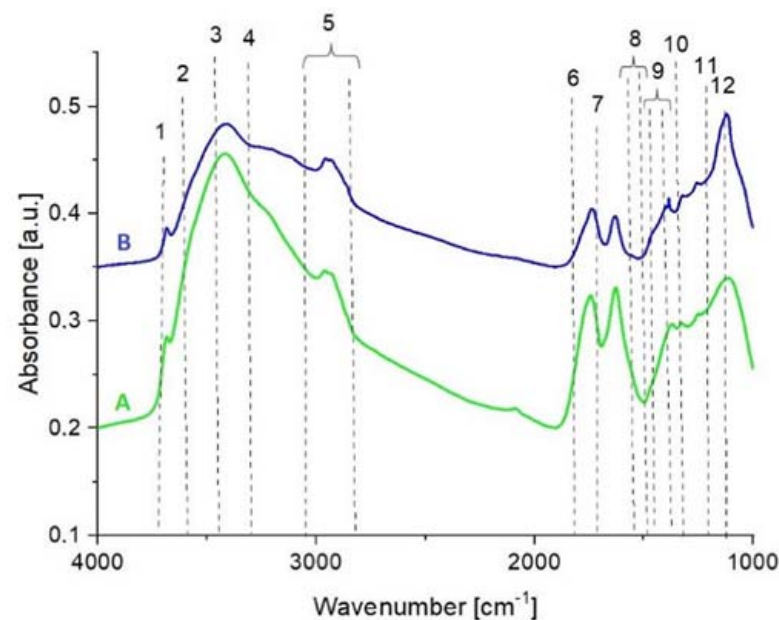
Figure 9. FTIR spectra of unmodified diamond nanoparticles DND (A), and plasma–chemically modified diamond nanoparticles MDP1 (B).

Table 4. Bond assignment of IR absorption bands in the spectral range 4000 cm^{-1} to 400 cm^{-1}.

No. in Fig. X	Vibrational Mode	Wavenumber (cm^{-1})	A	B
1	Stretching O–H (from isolated water)	3680	+	+
2	Stretching O–H (water on Lewis acid sites)	3640	−	−
3	Stretching O–H (like in alcohols or fenols)	3400	+	+
4	Stretching O–H (with strong intermolecular bonding	3290	+	+
5	Stretching CH_3 and CH_2 (asym and sym)	3000–2800	+	+
6	Stretching C=O (in esters)	1740	+	+
7	Stretching C=C	1630	+	+
8	Deformation CH_2 and CH_3	1480–1440	+	+
9	Stretching C–O (in carboxylic anhydride)	1385–1370	+	+
10	bending C–O (in ester)	1270–1250	+	+
11	Stretching C–O–C	1124	+	+
12	Stretching C–O–C	1080	−	−

4. Discussion and Conclusions

In the research presented above, modified and non-modified diamond nanoparticles do not show cytotoxic effect. Bacteriostatic effect against the bacterial strains used was observed in presence of both nanodiamonds. In the literature, a reference can be found that diamond nanoparticles with a special modification of functional groups are interpreted as bacteriostatic. However, it requires intentional modifications of the nanodiamond surface by attaching specific functional groups, and giving them anti-microbial properties [33].

The nanodiamond particles tested do not cause disruption of viability and, therefore, do not have cytotoxic effects on cells. Some publications show a comparison between modified and non-modified nanodiamonds. Hydroxylated nanodiamonds induce oxidative stress and are more cytotoxic than pure, un-modified detonation nanodiamond particles in human endothelial cells [34]. The comparison of the cytotoxicity of the unmodified DND powder and the plasma-chemically modified MDP1 powder shows the activity of the nanodiamond surface. Functionalization of nanodiamonds gives the possibility to obtain specific properties of nanodiamonds for biomedical applications.

Pure diamond nanoparticles (DND), also due to plasma-chemical modification (MDP1), do not show cytotoxicity. Analysis of the SEM results shows differences in the sizes and shapes of conglomerates of both modified and unmodified diamond nanoparticles. Plasma-chemical modification of diamond nanoparticles (MDP1) significantly affects the reduction of grain size (91.4 nm) and non-appearance of conglomerates as in the case of unmodified detonation powder (DND). X-ray diffraction (XRD) analysis shows that the modification of diamond nanoparticles had not changed its crystallographic structure. The results of Raman spectroscopy proved the higher content of diamond phase (ID/IG–1.24) in plasma-chemically modified detonation nanodiamond particles (MDP1) in comparison with pure detonation nanodiamond (DND). The plasma-chemical modification of nanodiamonds increases the content of the diamond phase and shows the carbonyl and hydroxyl groups under FT-IR spectroscopy, which significantly increase the reactivity of the diamond surface. FT-IR spectroscopy shows the presence of carbonyl groups (C=O) in the band at 1724 cm^{-1} in both modified and unmodified nanodiamonds. Plasma-chemically modified diamond nanoparticles synthesized by the detonation method (MDP1) are characterized by the highest content of hydroxyl groups (-OH groups); the wide peak at 3448 cm^{-1} is attributed to the O–H stretching vibration. In summary, independently from of the surface modification, diamond phase content, and grain size, nanodiamonds did not show any cytotoxic effect and showed bacteriostatic properties, which proves their high biocompatibility and the possibility of biomedical applications.

References

1. Danilenko, V.V. Nanodiamonds: Problems and prospects. *J. Superhard Mater.* **2010**, *32*, 301–310. [CrossRef]
2. Ceynowa, P.; Mitura, K.; Zinka, W.; Mitura, S. Diamond nanopowder modification system (DPP) in the rotating chamber of a plasma-chemical reactor (MW PACVD). *Elektronika* **2014**, *10*, 47–50.
3. Danilenko, V.V. On the history of the discovery of nanodiamond synthesis. *Phys. Solid State* **2004**, *46*, 595. [CrossRef]
4. Schrand, A.M.; Huang, H.; Carlson, C.; Schlager, J.J.; Osawa, E. Are diamond nanoparticles cytotoxic? *J.Phys. Chem B.* **2007**, *111*, 2–7. [CrossRef]
5. Mitura, K.; Kornacka, J.; Kopczyńska, E.; Kalisz, J.; Czerwińska, E.; Affeltowicz, M.; Kaczorowski, W.; Kolesińska, B.; Frączyk, J.; Bakalova, T. Active Carbon-Based Nanomaterials in Food Packaging. *Coatings* **2021**, *11*, 161. [CrossRef]
6. Niemiec, T.; Szmidt, M.; Sawosz, E.; Grodzik, M.; Mitura, K. The effect of diamond nanoparticles on redox and immune parameters in rats. *J. Nanosci. Nanotechnol.* **2011**, *11*, 9072–9077. [CrossRef]
7. Eivazzadeh-Keihan, R.; Maleki, A.; de la Guardia, M.; Bani, M.S.; Chenab, K.K.; Pashazadeh-Panahi, P.; Baradaran, B.; Mokhtarzadeh, A.; Hamblin, M.R. Carbon based nanomaterials for tissue engineering of bone: Building new bone on small black scaffolds: A review. *J. Adv. Res.* **2019**, *18*, 185–201. [CrossRef]
8. Chauhan, S.; Jain, N.; Nagaich, U. Nanodiamonds with powerful ability for drug delivery and biomedical applications: Recent updates on in vivo study and patents. *J. Pharm. Anal.* **2020**, *10*, 1–12. [CrossRef]
9. Zakrzewska, K.; Samluk, A.; Wierzbicki, M.; Jaworski, S.; Kutwin, M.; Sawosz, E.; Chwalibog, A.; Pijanowska, D.G.; Pluta, K.D. Analysis of the Cytotoxicity of Carbon-Based Nanoparticles, Diamond and Graphite, in Human Glioblastoma and Hepatoma Cell Lines. *PLoS ONE* **2015**. [CrossRef]
10. Zupančič, D.; Kreft, M.E.; Grdadolnik, M.; Mitev, D.; Iglič, A.; Veranič, P. Detonation nanodiamonds are promising nontoxic delivery system for urothelial cells. *Protoplasma* **2017**, *255*, 419–423. [CrossRef]
11. Norouzi, N.; Ong, Y.; Damle, V.G.; Najafi, M.B.H.; Schirhagl, R. Effect of medium and aggregation on antibacterial activity of nanodiamonds. *Mater. Sci. Eng. C* **2020**, *112*, 110930. [CrossRef] [PubMed]
12. Beranová, J.; Seydlová, G.; Kozak, H.; Benada, O.; Fišer, R.; Artemenko, A.; Konopásek, I.; Kromka, A. Sensitivity of bacteria to diamond nanoparticles of various size differs in gram-positive and gram-negative cells. *FEMS Microbiol. Lett.* **2014**, *351*, 179–186. [CrossRef] [PubMed]
13. Lišková, P.; Beranová, J.; Ukraintsev, E.; Fišer, R.; Kofroňová, O. Diamond nanoparticles suppress lateral growth of bacterial colonies. *Colloids Surf. B* **2018**, *170*, 544–552. [CrossRef] [PubMed]
14. Wehling, J.; Dringen, R.; Zare, R.N.; Maas, M.; Rezwan, K. Bactericidal Activity of Partially Oxidized Nanodiamonds. *ACS Nano* **2014**, *8*, 6475–6483. [CrossRef]
15. Jariwala, D.H.; Patel, D.; Wairkar, S. Surface functionalization of nanodiamonds for biomedical applications. *Mater. Sci. Eng. C* **2020**, *113*, 110996. [CrossRef]
16. Mitura, K.; Jędrzejewska-Szczerska, M.; Ceynowa, P.; Dudek, M.; Cicha, M. Hemokompatibility of non-functionalized and plasma-chemical functionalized detonation nanodiamond particles. *Arch. Metall. Mater.* **2015**, *60*, 73–79. [CrossRef]
17. Mitura, K.; Włodarczyk, E. Fluorescent Nanodiamonds in Biomedical Applications. *J. AOAC Int.* **2018**, *101*, 1297–1307. [CrossRef]
18. Bajpai, V.K.; Kamle, M.; Shukla, S.; Mahato, D.K.; Chandra, P.; Hwang, S.K.; Kumar, P.; Huh, Y.S.; Han, Y.-K. Prospects of using nanotechnology for food preservation, safety, and security. *J. Food Drug Anal.* **2018**, *26*, 1201–1214. [CrossRef]
19. Khaneghaha, A.M.; Hashemi, S.M.B.; Limbo, S. Antimicrobial agents and packaging systems in antimicrobial active food packaging: An overview of approaches and interactions. *Food Bioprod. Process.* **2018**, *111*, 1–19. [CrossRef]
20. Aliofkhazraei, M.; Ali, N.; Milne, W.I.; Ozkan, C.S.; Mitura, S. *Graphene Science Handbook*; CRC Press: Boca Raton, FL, USA, 2016.

21. Kurantowicz, N.; Sawosz, E.; Jaworski, S.; Kutwin, M.; Strojny, B.; Wierzbicki, M.; Szeliga, J.; Hotowy, A.; Lipińska, L.; Koziński, R. Interaction of graphene family materials with Listeria monocytogenes and Salmonella enterica. *Nanoscale Res. Lett.* **2015**, *10*, 23. [CrossRef]

22. Jaworski, S.; Sawosz, E.; Kutwin, M.; Wierzbicki, M.; Hinzmann, M.; Grodzik, M.; Winnicka, A.; Lipinska, L.; Wlodyga, K.; Chwalibog, A. In vitro and in vivo effects of graphene oxide and reduced graphene oxide on glioblastoma. *Int. J. Nanomed.* **2015**, *10*, 1585–1596. [CrossRef]

23. Maas, M. Carbon Nanomaterials as Antibacterial Colloids. *Materials* **2016**, *9*, 617. [CrossRef] [PubMed]

24. Szunerits, S.; Barras, A.; Boukherroub, R. Antibacterial Applications of Nanodiamonds. *Int. J. Environ. Res. Public Health* **2016**, *13*, 413. [CrossRef] [PubMed]

25. Plotnikov, V.A.; Makarov, S.V.; Bogdanov, D.G.; Bogdanov, A.S. The structure of detonation nanodiamond particles. In Proceedings of the 10th International Conference on Mechanics, Resource and Diagnostics of Materials and Structures, Ekaterinburg, Russia, 16–20 May 2016; AIP: New York, NY, USA, 2016. [CrossRef]

26. Mitura, K. HRTEM examinations of nanodiamond particles for biomedical application. *J. Achiev. Mater. Manuf. Eng.* **2009**, *37*, 317–322.

27. Bogdanov, D.; Plotnikov, V.; Bogdanov, A.; Makarov, S.; Vins, V.; Yelisseyev, A.; Lin, V.; Chepurov, A. Consolidation of nanocrystals of detonation diamonds at high-pressure high-temperature sintering. *Int. J. Refract. Met. Hard Mater.* **2018**, *71*, 101–105. [CrossRef]

28. Kryshtal, A.P.; Mchedlov-Petrossyan, N.O.; Laguta, A.N.; Kriklya, N.N.; Kruk, A.; Osawa, E. Primary detonation nanodiamond particles: Their core-shell structure and the behavior in organo-hydrosols. *Colloids Surf.A Physicochem. Eng. Asp.* **2020**, *614*, 126079. [CrossRef]

29. Korepanov, V.I.; Hamaguchi, H.; Osawa, E.; Ermolenkov, V.; Lednev, I.K.; Etzold, B.J.M.; Levinson, O.; Zousman, B.; Epperla, C.P.; Chang, H.-C. Carbon structure in nanodiamonds elucidated from Raman spectroscopy. *Carbon* **2017**, *121*, 322–329. [CrossRef]

30. Lambert, J.B. *Introduction to Organic Spectroscopy*; Macmillan: New York, NY, USA, 1987.

31. Kartick, B.S.; Srivastava, S.K.; Srivastava, I. Green Synthesis of Graphene. *J. Nanosci. Nanotechnol.* **2013**, *13*, 4320–4324. [CrossRef]

32. Ou, J.; Yan Bing, H.; Lan Zhen, H.; Zhang, R.; Xu, T.; Zhao, J. pH-sensitive nanocarriers for Ganoderma applanatum polysaccharide release via host–guest interactions. *J Mater Sci.* **2018**, *53*, 7963–7975. [CrossRef]

33. Kumaravel, V. Antimicrobial activity of menthol modified nanodiamond particles. *Chem. Eng. Sci.* **2021**, *416*, 129071. [CrossRef]

34. Solarska, K.; Gajewska, A.; Kaczorowski, W.; Bartosz, G.; Mitura, K. Effect of nanodiamond powders on the viability and prodution of reactive oxygen and nitrogen species in endothelial cells by unmodified and Fenton modified ultradisperse detonation diamond. *Diam. Relat. Mater.* **2012**, *21*, 9037–9046. [CrossRef]